Inhomogeneous Broadening Effect in THz Acoustic Cavities

G. Rozas,[1,*] B. Jusserand,[2] A. Fainstein,[1] and A. Lemaître[3]

[1]*Centro Atómico Bariloche & Instituto Balseiro, C.N.E.A., R8402AGP S. C. de Bariloche, Argentina*

[2]*Institut des Nanosciences de Paris, UPMC, CNRS UMR 7588, Campus Boucicaut, 75015 Paris, France*

[3]*Laboratoire de Photonique et de Nanostructures, CNRS, Route de Nozay, 91460 Marcoussis, France*

(Received April 12, 2010)

What is the lifetime of a cavity confined acoustic phonon in the relevant THz range, and what are its limiting factors, are questions of importance both from fundamental and device application perspectives. We present a model to study the effects of inhomogeneous broadening in planar acoustic cavities, separating the relative contributions of the superlattices and the cavity spacer. We contrast this model with ultra-high resolution Raman experiments in 1 THz semiconductor acoustic cavities and propose possible explanations for the discrepancies.

PACS numbers: 63.22.Np, 62.80.+f, 78.30.Fs

I. INTRODUCTION

Phonons in the THz-range have great importance both in basic research and in applications. THz coherent phonon sources could be used for nano-tomography [1, 2], to test fundamental properties of solid state systems at the nanometer scale [3], and, in a more general perspective, to control charge and light at THz frequencies through the electron-phonon interaction in many optoelectronic devices [4, 5]. One important device in this area is the planar phonon cavity, proposed less than ten years ago by Trigo *et al.* [6]. In close analogy to photon cavities one can foresee the use of phonon cavities as monochromatic sources of large strains for coherent phonon generation [7] and control [8, 9]. More importantly, drawing a parallel with vertical-cavity surface-emitting lasers (VCSEL) [10], planar phonon cavities could become the fundamental block providing the feedback mechanism for a phonon "lasing" device or SASER [11–15].

A phonon cavity consists of a spacer of width $n\lambda/2$ enclosed between two superlattices. Because of the acoustic impedance mismatch between the materials, the latter act as interference acoustic mirrors for the wavelength λ, emulating what distributed Bragg reflectors (DBR) do for light [16]. Like its photonic counterpart, phonon cavities are characterized by a highly monochromatic and amplified acoustic mode, with sound wavelengths of the order of a few nanometers [6]. Since their conception THz phonon cavities and the corresponding acoustic mode have been studied by Raman scattering [6, 17], and their acoustic transmission has been measured in the temporal domain by femtosecond pump-

and-probe techniques [18]. Quasi-monochromatic coherent phonon generation using a 0.6 THz phonon cavity has also been demonstrated [19]. On the other hand, some questions about the ultimate quality that can be achieved on these devices were addressed recently in Ref. [20].

The quality of a cavity is given by its Q-factor $Q = \lambda/\Delta\lambda$, where $\Delta\lambda$ is the full-width at half-maximum (FWHM) of the cavity mode peak in the acoustic transmission of the system. The theoretical Q-factor of an acoustic cavity can be controlled through the reflectivity of the acoustic mirrors, being larger for higher reflectivities. It is also closely related to the lifetime of the cavity phonons, which live longer in the cavity region as the reflectivity of the mirrors increases. From an applied point of view high quality cavities and long phonon lifetimes are essential if one expects acoustic cavities to play in a SASER the same role that optical cavities play in a VCSEL. Theoretically at least, Q-factors on the order of 10^4 and lifetimes of several nanoseconds should be attainable in cavities grown by molecular beam epitaxy (MBE). However, in spite of the many similarities connecting light and sound, two crucial differences arise when dealing with phonons in the THz range. On the one hand, phonons are intrinsically anharmonic [21, 22]. In contrast to photons, a phonon will always decay into two or more phonons or will collide with a phonon present in the thermal bath, and this is more probable the larger the phonon energy and the higher the temperature [23, 24]. On the other hand, for phonons of $\lambda \sim 5$ nm the required surface quality would be challenging even for the best state-of-the-art MBE, leading to a possible strong interaction of phonons with surface imperfections in most of the structures.

The practical limitations to the lifetime and consequently to the minimum linewidth and maximum amplification that can be achieved in these cavities are then important matters for device applications. Experimental and theoretical work has been done in the area of thermal conductivity of nanostructures taking into account both anharmonic decay and interface defects [25, 26]. Bulk acoustic phonon propagation and attenuation in the GHz range have been tested by picosecond ultrasonics as a function of temperature [24]. Optical phonon Raman experiments in bulk have been compared with anharmonic lifetime ab initio calculations [27] and very long lifetimes have been demonstrated with time resolved optical techniques in bulk ZnO [28]. Neutron spin-echo has also been shown to be a powerful tool to study non dispersive phonon lifetimes in bulk materials [29]. Finally, the effect of surface roughness in the reflection of acoustic waves at an air/solid interface has been studied by a femtosecond transient transmission technique in piezoelectric materials [30]. All theses reports show that both the bulk phonon lifetime and the scattering at interfaces and defects should be taken into account to properly approach the problem. In this paper we will study the possible effects of inhomogeneous broadening in the linewidth of the acoustic cavity mode, separating the relative contributions of the superlattices and the cavity spacer.

II. MODELLING THE INHOMOGENEOUS BROADENING

In a recently published paper we have taken the approach of directly studying the lifetime of THz acoustic cavities by means of an ultra-high resolution Raman scattering

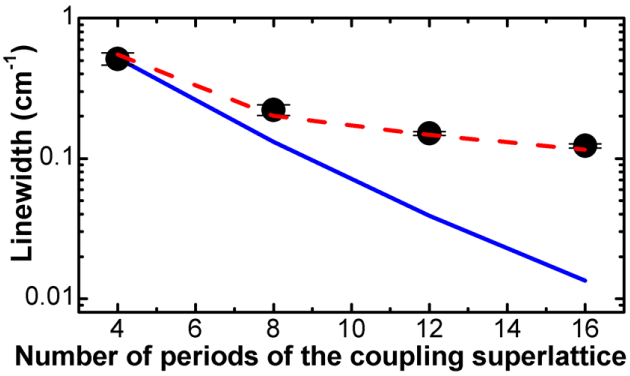

FIG. 1: Dependence of the experimental (full circles), calculated nominal (full line), and calculated with inhomogeneous broadening (dashed line) Raman linewidth of the acoustic cavity mode for a $3\lambda/2$ 1 THz cavity, as a function of the reflectivity of the mirror coupling the cavity to the substrate [20].

technique specially developed for those experiments [20, 31]. A set of four GaAs/AlAs $3\lambda/2$ acoustic cavities with a mode frequency of 1 THz grown by MBE were studied. The coupling of the acoustic cavity spacer to the substrate was done through a superlattice (SL) that had a different number of periods in each sample (4 to 16), effectively changing its performance as a phonon mirror. This variation modified the nominal Q-factor of the acoustic cavities, spanning a range $63 < Q < 2400$. This meant that the cavity mode could tunnel through this bottom superlattice to the substrate at theoretical lifetimes that varied from 10 ps for the 4-period sample to 390 ps for the 16-period one. To test these theoretical values we took advantage of the close relationship between the lifetime of the acoustic cavity mode and the linewidth of the corresponding Raman scattering peak. It can be shown that if the former is τ, then the latter will be FWHM $= 1/(2\pi\tau)$. In this case, the equivalent calculated Raman linewidths for the cavity mode varied from 0.52 to 0.014 cm^{-1}. Figure 1 shows the relevant result for this article: while the theoretical linewidth (full line) decreased exponentially with the number of periods of the coupling superlattice, the experimental linewidth (full circles) had a saturating behaviour, with a lower limit at $\sim$0.1 cm^{-1}. Further experiments showed that this effect was almost temperature independent, ruling out anharmonicity as the main contribution to the broadening of the acoustic cavity mode Raman peak [20]. To explain this saturation in the minimum Raman linewidth of the acoustic cavity mode we have put forward an inhomogeneous broadening model including fluctuations in the thickness of the layers forming the acoustic cavity (dashed line).

Raman scattering cross section can be calculated theoretically for arbitrary structures by means of a continuous photoelastic model that takes into account the modulation in elastic properties, photoelastic constant and refractive index introduced by the different materials forming the structure [32, 33]. Using the average layers thickness from X-ray measurements, a nominal spectrum can be calculated. The acoustic cavity mode Raman peak for this nominal structure is shown in Fig. 2 in thick full line. In order to introduce an

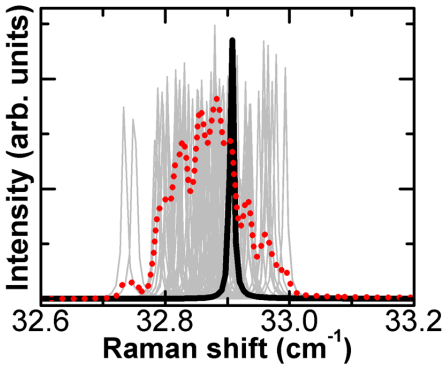

FIG. 2: Inhomogeneous broadening of an acoustic cavity mode Raman peak. Spectra for slightly different structures (thin full line) are generated introducing random thickness fluctuations in the nominal structure (thick full line). The final broadened spectrum (dotted line) is obtained by averaging the former.

inhomogeneous broadening into the simulation we take this average structure, defined by the size d_i of each layer (being i the number of the layer), and shift the interface between each pair of layers by an amount $\delta_{i,i+1}$. After the modification the widths of the layers become $d'_i = d_i + (\delta_{i,i+1} - \delta_{i-1,i})$, creating a slightly modified structure. Note that by introducing the fluctuations in this way we make sure that both the total size of the structure and the average period of the superlattices remain constant and compatible with the X-ray data. The $\delta_{i,i+1}$ are taken to be random numbers with a certain distribution. The next step in the simulation is to produce a large number of these modified structures, calculating the Raman spectrum for each one of them (thin full lines in Fig. 2). The final homogeneously broadened Raman spectrum is obtained by averaging several thousands of these spectra (dashed line for 100 spectra). For this work we have tested two different random distributions for $\delta_{i,i+1}$: a Gaussian distribution and a Laplace distribution. For the structures studied here we have found that a Laplace distribution $P(\delta_{i,i+1}) = \exp(-|\delta_{i,i+1}/\alpha|)/(2\alpha)$ results in broadened spectra that better reproduce the experimental Lorentzian line shape of the acoustic cavity mode. This is the distribution that will be used through this article.

The only free parameter on this model is the typical size α of the fluctuations, which can be obtained by fitting the experimental data on Fig. 1. A value of $\alpha = 0.06$ nm (1/9th of a unit cell) reproduce very well the observed behaviour (dashed line). In view that the cavity mode is spatially localized predominantly at the cavity spacer, with some penetration into the mirrors [6], we have looked separately at the contributions to the broadening coming from the superlattices and from the cavity spacer. This was done by repeating the described procedure, but setting $d'_i = d_i$ constant in the relevant layers. The result for a $3\lambda/2$ 1THz is shown in Fig. 3: approximately 60% of the broadening is produced by the fluctuations in the superlattices (full rectangle), the rest coming from the cavity spacer (empty rectangle). Although in both cases the broadening is produced by a shift in the Raman peak, the origin of this shift is different for each case. While a change in the size of the cavity spacer

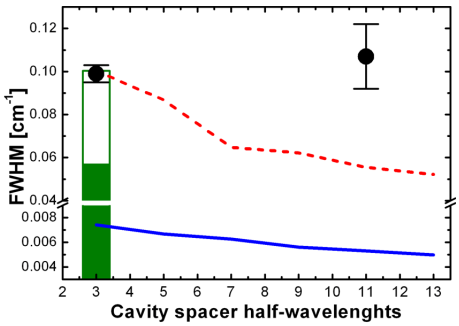

FIG. 3: Experimental linewidth of the acoustic cavity mode Raman peak for a 1 THz cavity as a function of the size of the cavity spacer (full circles) and prediction from the thickness fluctuations model (dashed line). The nominal linewidth (full line) and the contributions to the broadening coming from the superlattice (full rectangle) and the cavity spacer (empty rectangle) are also included. Note the changed scale of the vertical axis.

directly affects the resonant wavelength and, consequently, changes the energy of the mode, the fluctuations in the mirrors enter in a more indirect way. Being interference mirrors, deviations from perfect periodicity affect the phase of the acoustic wave that is reflected. That in turn modifies the resonant condition for the width of the cavity spacer to be not exactly an integer number of half wavelengths, which shifts the peak.

As stated in the introduction of this article, the ideal system for applications would be one in which the linewidth of the mode is as low as possible at the highest energy possible. The fact that a significant part of the broadening comes from the cavity spacer itself presents a simple solution to decrease the linewidth of the acoustic mode while maintaining its energy. The idea is presented in Fig. 3: by increasing the size of the cavity spacer from $3\lambda/2$ to $13\lambda/2$, and within the inhomogeneous broadening model, the relative weight of the fluctuations in the spacer for a fixed α diminishes, reducing the expected linewidth to the half (dashed line).

III. EXPERIMENTAL TEST AND CONCLUSIONS

In order to test this prediction a new 1 THz acoustic cavity was grown by MBE, in this case having an $11\lambda/2$ spacer as opposed to the $3\lambda/2$ cavities described in Ref. [20]. Besides this enlargement of the cavity spacer and the addition of an optical DBR on top of the sample to enhance the Raman signal through optical resonance [34, 35], this sample is identical to the 16 periods cavity described in that article. The acoustic mirrors are 16-period 3.5/1.5 nm GaAs/AlAs superlattices, enclosing a 26 nm GaAs cavity spacer. Back-scattering Raman experiments where performed at liquid nitrogen temperature using the same ultra-high resolution experimental setup used in Ref. [20] and described in more detail in Ref. [31]. Laser excitation was set at 860 nm, 60 meV below the absorption of the GaAs substrate at that temperature, and a double optical resonance configuration was

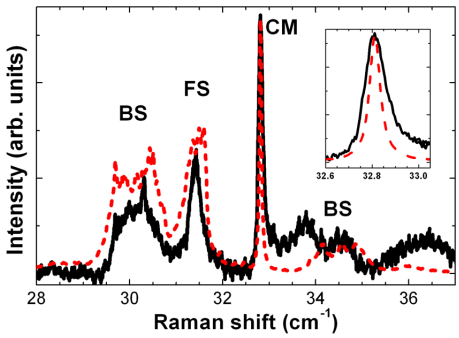

FIG. 4: Experimental Raman spectrum (full line) for an $11\lambda/2$ 1THz acoustic cavity. The inset shows a detail of the cavity mode peak. The theoretical spectrum (dashed line) was simulated with the thickness fluctuations model and using the same parameters as in Fig. 1.

used [35].

Figure 4 shows a comparison of the experimental Raman spectrum (full line) and the spectrum predicted by the model described in the previous section (dashed line), using the α parameter obtained for the $3\lambda/2$ samples. The acoustic cavity mode (CM), and the $q = 0$ ("forward"-scattering, FS) and $q = 2k$ ("back"-scattering, BS) modes of the superlattices, where $q(k)$ is the phonon (photon) wave-vector, are identified. A detailed view of the cavity mode peak is included in the inset. Although the calculation correctly predicts the main features of the spectrum like the position and line shape of the modes, it clearly fails to account for the full linewidth of the cavity mode. If we include this new experimental point in Fig. 3 (rightmost full circle) we can see not only that the model is underestimating the real linewidth, but also that there does not seem to be a change, within the experimental uncertainty, in the experimental result when passing from $3\lambda/2$ to $11\lambda/2$.

A possible explanation for this discrepancy could be related to the sample having a poorer quality than the ones studied previously, in which case using the same α parameter would be the wrong choice. Further studies trough X-ray and photoluminescence are necessary to rule out this possibility. On the other hand, if the samples have approximately the same quality and the model presented needs a reformulation, the clear message to be taken from this experiment would be that the main contribution to the broadening is coming from the mirrors. A good candidate to introduce broadening independent of the size of the acoustic spacer is scattering at interface defects, which would introduce an homogeneous broadening to the cavity mode [25, 26]. New experiments changing the energy of the confined phonons should be able to assess the relation between homogeneous and inhomogeneous broadening on these cavities and their relative contributions to the total linewidth of the mode.

References

* Electronic address: rozasg@ib.cnea.gov.ar

[1] K.-H. Lin, C.-T. Yu, S.-Z. Sun, H.-P. Chen, C.-C. Pan *et al.*, Appl. Phys. Lett. **89**, 043106 (2006).
[2] K.-H. Lin, C.-M. Lai, C.-C. Pan, J.-I. Chyi, J.-W. Shi *et al.*, Nature Nanotech. **2**, 704 (2007).
[3] K. Sokolowski-Tinten, C. Blome, J. Blums, A. Cavalleri, C. Dietrich *et al.*, Nature **422**, 287 (2003).
[4] K.-H. Lin, G.-W. Chern, Y.-K. Huang, and C.-K. Sun, Phys. Rev. B **70**, 073307 (2004).
[5] A. Akimov, A. Scherbakov, D. R. Yakovlev, C. T. Foxon *et al.*, Phys. Rev. Lett. **97**, 037401 (2006).
[6] M. Trigo, A. Bruchhausen, A. Fainstein, B. Jusserand *et al.*, Phys. Rev. Lett. **89**, 227402 (2002).
[7] N. D. Lanzillotti-Kimura, A. Fainstein, A. Huynh, B. Perrin *et al.*, Phys. Rev. Lett. **99**, 217405 (2007).
[8] A. Bartels, T. Dekorsy, H. Kurz, and K. Koöhler, Appl. Phys. Lett. **72**, 2844 (1998).
[9] Ü. Özgür, C.-W. Lee, and H. O. Everitt, Phys. Rev. Lett. **86**, 5604 (2001).
[10] K. Iga, Jpn. J. Appl. Phys. **47**, 1 (2008).
[11] P. A. Fokker, J. I. Dijkhuis, and H. W. de Wijn, Phys. Rev. B **55**, 2925 (1997).
[12] L. G. Tilstra, A. F. M. Arts, and H. W. de Wijn, Phys. Rev. B **76**, 024302 (2007).
[13] A. J. Kent, R. N. Kini, N. M. Stanton, M. Henini *et al.*, Phys. Rev. Lett. **96**, 215504 (2006).
[14] R. P. Beardsley, A. V. Akimov, M. Henini, and A. J. Kent, Phys. Rev. Lett. **104**, 085501 (2010).
[15] I. S. Grudinin, H. Lee, O. Painter, and K. J. Vahala, Phys. Rev. Lett. **104**, 083901 (2010).
[16] V. Narayanamurti, H. L. Störmer, M. A. Chin, A. C. Gossard *et al.*, Phys. Rev. Lett. **43**, 2012 (1979).
[17] P. Lacharmoise, A. Fainstein, B. Jusserand, and V. Thierry-Mieg, Appl. Phys. Lett. **84**, 3274 (2004).
[18] A. Huynh, N. D. Lanzillotti-Kimura, B. Jusserand *et al.*, Phys. Rev. Lett. **97**, 115502 (2006).
[19] M. F. Pascual Winter, G. Rozas, A. Fainstein *et al.*, Phys. Rev. Lett. **98**, 265501 (2007).
[20] G. Rozas, M. F. Pascual Winter, B. Jusserand *et al.*, Phys. Rev. Lett. **102**, 015502 (2009).
[21] P. G. Klemens, J. Appl. Phys. **38**, 4573 (1967).
[22] S. Tamura, Phys. Rev. B **31**, 2574 (1985).
[23] C. Herring, Phys. Rev. **95**, 954 (1954).
[24] W. Chen, H. J. Maris, Z. R. Wasilewski, S. Tamura, Philos. Mag. B **70**, 687 (1994).
[25] W. S. Capinski, H. J. Maris, T. Ruf, M. Cardona, K. Ploog *et al.*, Phys. Rev. B **59**, 8105 (1999).
[26] B. C. Daly, H. J. Maris, K. Imamura, and S. Tamura, Phys. Rev. B **66**, 024301 (2002).
[27] C. Ulrich, E. Anastassakis, K. Syassen, A. Debernardi *et al.*, Phys. Rev. Lett. **78**, 1283 (1997).
[28] C. Aku-Leh, J. Zhao, R. Merlin, J. Menéndez, and M. Cardona, Phys. Rev. B **71**, 205211 (2005).
[29] J. Kulda, A. Debernardi, M. Cardona, F. de Geuser *et al.*, Phys. Rev. B **69**, 045209 (2004).
[30] C.-L. Hsieh, K.-H. Lin, S.-B. Wu, C.-C. Pan, J.-I. Chyi *et al.*, Appl. Phys. Lett. **85**, 4735 (2004).
[31] G. Rozas, M. F. Pascual Winter, B. Jusserand, A. Fainstein *et al.*, AIP Conf. Proc. **1199**, 169 (2010).
[32] J. He, B. Djafari-Rouhani, and J. Sapriel, Phys. Rev. B **37**, 4086 (1988).
[33] A. Bruchhausen, PhD. Thesis (Instituto Balseiro, Argentina, 2008).
[34] A. Fainstein, B. Jusserand, and V. Thierry-Mieg , Phys. Rev. B **53**, R12387 (1996).
[35] A. Fainstein and B. Jusserand, Phys. Rev. B **57**, 2402 (1998).